Monthly Notices
of the
ROYAL ASTRONOMICAL SOCIETY

MNRAS **458,** 3394–3398 (2016)
Advance Access publication 2016 March 2

doi:10.1093/mnras/stw492

Prediction of transits of Solar system objects in *Kepler*/K2 images: an extension of the Virtual Observatory service SkyBoT

J. Berthier,[1]★ B. Carry,[1,2]★ F. Vachier,[1] S. Eggl[1] and A. Santerne[3]★

[1]*IMCCE, Observatoire de Paris, PSL Research University, CNRS, Sorbonne Universités, UPMC Univ Paris 06, Univ Lille, France*
[2]*Laboratoire Lagrange, Université de Nice-Sophia Antipolis, CNRS, Observatoire de la Côte d'Azur, France*
[3]*Instituto de Astrofísica e Ciências do Espaço, Universidade do Porto, CAUP, Rua das Estrelas, P-4150-762 Porto, Portugal*

Accepted 2016 February 26. Received 2016 February 23; in original form 2016 February 4

ABSTRACT

All the fields of the extended space mission *Kepler*/K2 are located within the ecliptic. Many Solar system objects thus cross the K2 stellar masks on a regular basis. We aim at providing to the entire community a simple tool to search and identify Solar system objects serendipitously observed by *Kepler*. The sky body tracker (SkyBoT) service hosted at Institut de mécanique céleste et de calcul des éphémérides provides a Virtual Observatory compliant cone search that lists all Solar system objects present within a field of view at a given epoch. To generate such a list in a timely manner, ephemerides are pre-computed, updated weekly, and stored in a relational data base to ensure a fast access. The SkyBoT web service can now be used with *Kepler*. Solar system objects within a small (few arcminutes) field of view are identified and listed in less than 10 s. Generating object data for the entire K2 field of view (14°) takes about a minute. This extension of the SkyBoT service opens new possibilities with respect to mining K2 data for Solar system science, as well as removing Solar system objects from stellar photometric time series.

Key words: virtual observatory tools – ephemerides – planetary systems.

1 INTRODUCTION

The NASA Discovery mission *Kepler* was launched in 2009, with the aim of detecting exoplanets from the photometric signature of their transit in front of their host star (Borucki et al. 2009). Following the second failure of a reaction wheel in 2013 May, the original field of view (FoV) in Cygnus could not be fine pointed anymore. An extension of the mission, dubbed K2 (Howell et al. 2014), was designed to be a succession of 3-month long campaigns, where the spacecraft's FoV scans the ecliptic plane. This mode of operations implies that many Solar system objects (SSOs) cross the subframes centred on K2 mission targets. Following a visual inspection of the K2 engineering FoV, Szabó et al. (2015) reported that SSOs had crossed half of the 300 stars monitored over the 9 d of engineering observations.

Owing to the large number of stellar targets in each K2 campaign, the likelihood of observing SSOs at any single epoch is indeed high. Given a typical mask size around each target of 15 × 15 pixels or 1 × 1 arcmin for between 10 000 and 30 000 stellar targets, the filling factor[1] of K2 entire FoV ranges from 3 per cent to 10 per cent (Table 1). A corresponding fraction of the SSOs that cross K2 FoVs are within a target mask at each instant, from a few tens of minutes for a near-Earth object to approximately 6 h for a main-belt asteroid, and up to several days for a Trojan or a transneptunian object. Over a whole campaign, the cumulative probability to observe these SSOs get close to one, as the different target masks, stacked over ecliptic longitude, almost fill entirely the range of ecliptic latitudes within K2 FoVs (Table 1). Each SSO has thus only a few per cent chance to dodge all the target masks as it crosses K2 FoV (Table 1). Several programmes dedicated to planetary science have been already carried out by K2, like characterization of the rotation period of transneptunian objects (Pál et al. 2015). The giant planet Neptune and its satellites were also observed in C3, and Uranus will be in C8.

Considering the typical magnitude of K2 stellar targets (80 per cent of the stars have a $V \leq$ 15–16), and the typical K2 photometric precision of a few hundreds ppm, many SSOs will be imaged together with the stars. At any instant several thousands of SSOs with $V \leq 20$ lay within K2 entire FoV (e.g. Fig. 1). An asteroid of 20th magnitude will contribute to the star signal at a level of 1000 ppm, and is, therefore, easily detectable.

There is a twofold interest in having a simple tool to predict *encounters* between stars and SSOs:

(i) The K2 community profits from identifying any encounters that add undesirable signals, hence photon noise, to stellar light curves, at non-negligible levels.

★ E-mail: berthier@imcce.fr (JB); benoit.carry@oca.eu (BC); alexandre.santerne@astro.up.pt (AS)

[1] The fraction of the K2 FoV that is actually downlinked.

Table 1. Number of K2 stellar targets, fraction of the total field of view downlinked to Earth, filling fraction of ecliptic latitudes (β_f), expected average number and standard deviation of stellar encounters for each SSO (μ_e and σ_e), for each campaign (up to C7).

Campaign	Targets	Area (per cent)	β_f (per cent)	μ_e	σ_e
C0	7756	2.90	94.16	4.3	2.7
C1	21 647	8.09	98.25	11.8	5.4
C2	13 401	5.01	96.53	7.4	4.4
C3	16 375	6.12	97.94	9.1	4.8
C4	15 781	5.90	98.18	8.7	4.2
C5	25 137	9.40	98.68	13.8	6.3
C6	27 289	10.20	98.91	14.9	6.2
C7	13 261	4.96	96.74	7.3	4.9

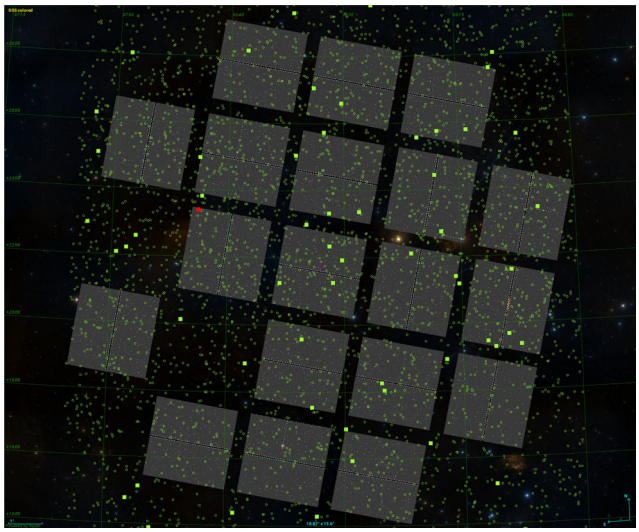

Figure 1. K2 full frame image taken on 2014 March 11, at 23:27:23.77 UTC (mid-exposure), overplotted on the DSS coloured view, displayed by Aladin. All the 3136 known SSOs brighter than $V \leq 20$ (among 9702) present within the FoV reported by SkyBoT are represented, by the green circles for asteroids (and solid squares for $V \leq 16.5$), and by the red dot for a comet (84P, $V = 18.8$).

(ii) The Solar system community profits, as each encounter provides a short light curve (typical a couple of hours) of an SSO with excellent photometric accuracy. On average, 10 encounters per campaign can be expected (Table 1).

To cater to those demands, we present an extension of our Virtual Observatory (VO) tool sky body tracker (SkyBoT) (Berthier et al. 2006), hosted at Institut de mécanique céleste et de calcul des éphémérides (IMCCE). This tool is web based, open-access, and provides a simple way to identify all the SSOs present within a FoV at a given epoch. This paper is organized as following: in Section 2, we describe the SkyBoT service, its algorithm and access, and we show a pair of examples in Section 3.

2 SKYBOT: THE VO SKY BODY TRACKER

The typical queries to astronomical catalogues are so-called *cone searches*, in which all targets within a given FoV are returned. This is mostly adapted to objects with fixed coordinates, such as stars and galaxies, their parallax and proper motion being much smaller than the FoV. But the coordinates of objects in our Solar system constantly change and cone searches cannot use pre-defined catalogues. As a result, most tools for source identification fail to associate the observed SSO with a known source. The SkyBoT service provides a solution by pre-computing ephemerides of all the known SSOs, and storing them in a relational data base for rapid access upon request.

2.1 Ephemerides computation and SkyBoT algorithm

Among other services, the IMCCE produces the French national ephemerides under the supervision of the Bureau des longitudes. The development and maintenance of ephemerides tools for the astronomical community is also a part of its duties. As such, the institute offers online computation of SSO ephemerides through a set of web services.[2]

The ephemerides of planets and small SSOs are computed in the ICRF quasi-inertial reference frame taking into account perturbations of the eight planets, and post-Newtonian corrections. The geometric positions of the major planets and the Moon are provided by INPOP planetary theory (Fienga et al. 2014). Those of small SSOs (asteroids, comets, Centaurs, transneptunian objects) are calculated by numerical integration of the *N*-body perturbed problem (Gragg–Bulirsch–Stoer algorithm, see Bulirsch & Stoer 1966; Stoer & Bulirsch 1980), using the latest published osculating elements, from the `astorb` (Bowell, Muinonen & Wasserman 1993) and `cometpro` (Rocher & Cavelier 1996) data bases. The overall accuracy of asteroid and comet ephemerides provided by our services are at the level of tens of milliarcseconds, mainly depending on the accuracy of the minor planet's osculating elements. The positions of natural satellites are obtained thanks to dedicated solutions of their motion, e.g. Lainey, Duriez & Vienne (2004a), Lainey, Arlot & Vienne (2004b), Lainey, Dehant & Pätzold (2007) for Mars and Jupiter, Vienne & Duriez (1995) for Saturn, Laskar & Jacobson (1987) for Uranus, and Le Guyader (1993) for Neptune's satellites.

The ephemerides of all the known objects of our Solar system are recomputed on a weekly basis, for a period which extends from the end of the 19th century (1889 November 13) to the first half of the 21st century (2060 March 21), and stored with a time step of 10 d in a hierarchical tree structure supported by nodes based on geocentric equatorial coordinates. For each cone search, this data base is queried, and all the targets expected to be within the FoV are listed. Their topocentric ephemerides for the exact requested time are then computed on the fly.

The apparent topocentric celestial coordinates (i.e. relative to the true equator and equinox of the date) are computed by applying light aberration, precession, and nutation corrections to the observer–target vector. The coordinates of the topocentre can either be provided directly by users (longitude, latitude, altitude), or by using the observatory code provided by IAU Minor Planet Center[3] for listed observatories.

The SkyBoT service was released in 2006 (Berthier et al. 2006). It is mostly used to identify moving objects in images (e.g. Conrad et al. 2009; Delgado, Delmotte & Vuong 2011; Carry et al. 2012; Bouy et al. 2013), and data mining of public archives (e.g. Vaduvescu et al. 2009, 2011, 2013; Carry et al. 2016). It responds to about 80 000 requests every month (more than 18 millions in 7 yr),

[2] http://vo.imcce.fr/webservices/
[3] http://www.minorplanetcenter.net/iau/lists/ObsCodesF.html

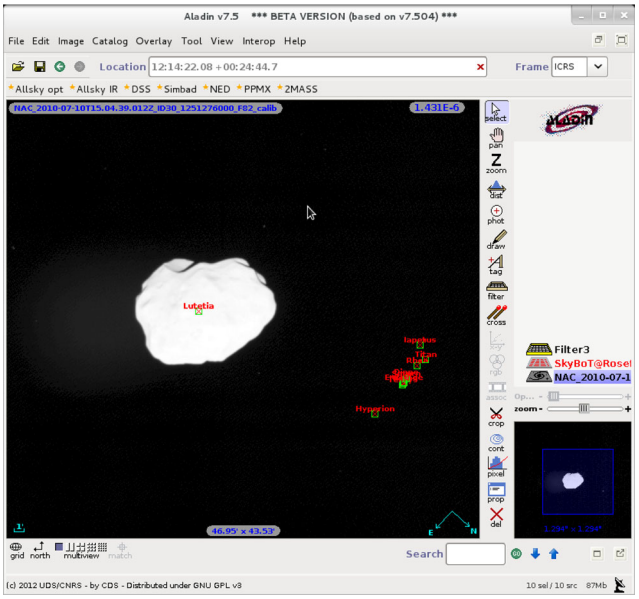

Figure 2. OSIRIS NAC image taken during the flyby of asteroid (21) Lutetia by ESA *Rosetta* space mission, on 2010 July 10, at 15:04:30 UTC (Sierks et al. 2011), displayed in Aladin. A SkyBoT cone-search query correctly lists Lutetia, together with Saturn and its satellites imaged in the background. Considering their dramatic difference of distance to *Rosetta* (36 000 km and 6.8 au, respectively), this example validates the SkyBoT upgrade to space missions.

and has a typical response time of less than 10 s for 95 per cent of requests.

2.2 An extension to non-Earth-bound geometries

Owing to the large number of known SSOs (currently 700 000), and the extended period of time that needs to be covered (from the first photographic plates to the present), pre-computations are the key to a timely service. As the data base of pre-computed ephemerides was ordered in a tree based on equatorial coordinates (RA/Dec.) to allow quick identification of potential targets within a FoV, the service was limited to a single geometry. The large parallax presented by objects within the Solar system indeed implies different equatorial coordinates depending on the position of the observer. The first releases of SkyBoT were thus limited to Earth geocentre, topocentres, and low-orbit satellites such as the *Hubble Space Telescope* or the International Space Station.

In 2010, we started a new phase of the SkyBoT development to allow the use of its cone-search method from other geometries. This was motivated by availability of wide-field ($2^\circ \times 2^\circ$ and $10^\circ \times 10^\circ$) images taken by the OSIRIS camera on-board the ESA *Rosetta* mission, which is on an interplanetary trajectory crossing the asteroid main-belt, between Mars and Jupiter. The great distance between the probe and the Earth, combined with the proximity of SSOs implied observing geometries so different that the Earth-bound data base could not be used to search for and identify targets correctly. This challenge was recently solved. An example validating the corresponding update of the SkyBoT service is presented in Fig. 2.

To preserve the fast response time of the service, a switch was set in place, to redirect queries to different data bases, one for each space probe. These data bases have smaller time coverage, corresponding only to the mission lifetimes. The weekly computation of ephemerides is, therefore, not as CPU intensive as for the main (Earth) data base. There are currently two space probes available: *Rosetta* and *Kepler*. The architecture of SkyBoT after the update is such that we can add more space probes upon request: any space mission located on a Earth leading or trailing orbit (e.g. *Herschel*), or at L2 point (e.g. JWST, *Euclid*), or on an interplanetary trajectory (e.g. *Cassini*, JUNO) could be added, if desired by the community.

2.3 Access to the service

There are several ways to use the SkyBoT web service. Users who may want to discover the service can use a simple query form on the IMCCE's VO SSO portal[4] or the well-established Aladin Sky Atlas (Bonnarel et al. 2000). The service is also fully compliant with VO standards, and thus, can be scripted in two different ways: (i) by writing a client to send requests to the SkyBoT server and to analyse the response, or (ii) by using a command-line interface and a data transfer program such as CURL or WGET.

In all cases, three parameters must be passed to SkyBoT: the pointing direction (RA/Dec.), the epoch of observation, and the size of the FoV. The typical response time for request from K2 point of view are of a few seconds for small FoV (target mask), and of about 1 min for the entire FoV of *Kepler* of about 14°.

3 SOME EXAMPLES

We now present a couple of examples of the typical usage of the SkyBoT service for K2. In Fig. 1, we show a full frame image from C0, together with the result of a SkyBoT request: among the 9702 SSOs located in the FoV at that time, 3136 are brighter than $V \leq 20$, and about 50 are brighter than $V \leq 16$, thus potentially observable by K2. In Fig. 3, we present the light curve of the star EPIC 201872595 ($K_p = 12.2$) from Campaign #1, in which each surge of flux is caused by the transit of a different SSO within the target mask. The stellar flux is clearly contaminated by the SSOs. This is an obvious case of transits by SSOs, each being barely less bright ($V \sim 14$–15) than the target star. Fainter SSOs ($V \sim 18$–19) still affect stellar light curves, without being easily identifiable by naked eye. Using the SkyBoT service, it is easy to check any suspicious point in a stellar light curve, by performing a cone search, centred on the star, at the time of the corresponding photometry measurement, with a narrow FoV of a few arcseconds corresponding to the apparent size of the stellar mask.

The service also allow us to hunt for photometric data of SSOs. One can use SkyBoT to get the list of all the SSOs within the K2 entire FoV for each campaign, and compute their encounters with target stars to extract their photometry. For the fast generation of detailed ephemerides for each target, we recommend the use of our Miriade service (Berthier et al. 2009). Requesting SkyBoT cone search for the entire FoV, with a time step of 30 min during a whole campaign, is more CPU intensive than computing the same ephemerides for only the identified targets with Miriade.

In Fig. 4, we present 10 light curves of asteroid (484) Pittsburghia (apparent magnitude ∼15) we measured in K2 Campaign #0. The light curves have been constructed following the steps described above: a global SkyBoT request, followed by a Miriade generation of ephemerides every 30 min for Pittsburghia, and finally a check of whenever the asteroid was within one of the stellar masks. The synthetic light curve was generated using the 3D shape model of Pittsburghia by Durech et al. (2009) and Hanuš et al. (2011) is

[4] http://vo.imcce.fr

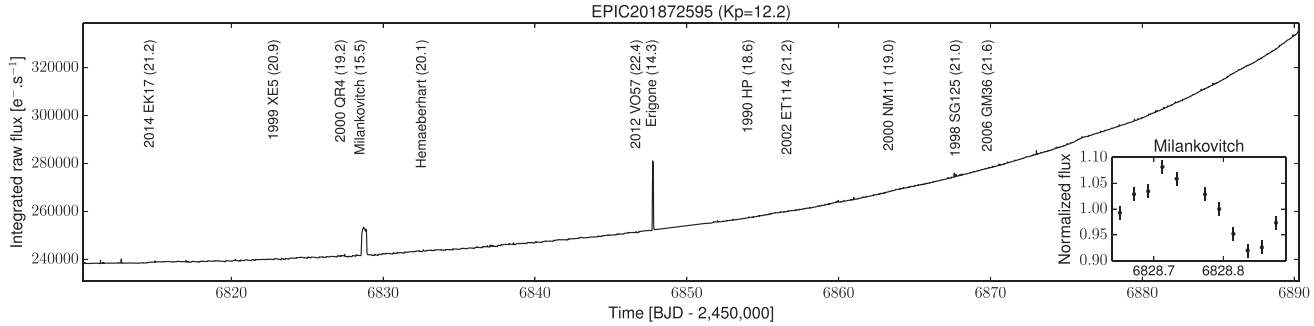

Figure 3. K2 raw light curve integrated overall pixels of the target EPIC 201872595 ($K_p = 12.2$) observed during Campaign #1. The increase in flux along the campaign is a systematic effect. The predicted transits of known SSOs down to a magnitude of 22.5 are indicated together with their expected V magnitude. The transit of two relatively bright SSOs, (1605) Milankovitch and (163) Erigone, are clearly visible. The fainter SSOs also imprint a significant increase in the observed flux as they pass into the target imagette. The inset in the bottom right is a zoom on the transit of (1605) Milankovitch. It displays the target-corrected and normalized flux of the SSO, and highlights the phase rotation of the SSO.

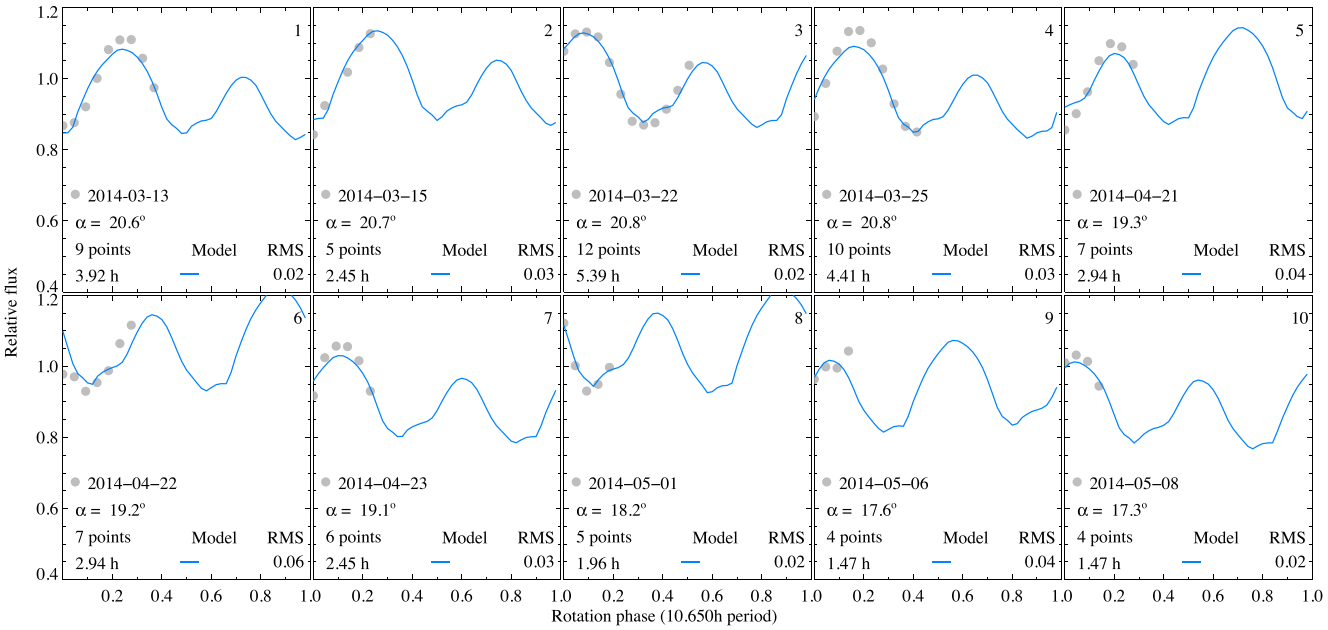

Figure 4. Example of asteroid light curves retrieved from K2 images. The grey dots represent the measured photometry of (484) Pittsburghia, and the blue curves stand for the synthetic light curves obtained from the 3D shape model of the asteroid by Durech et al. (2009) and Hanuš et al. (2011). The residuals between observed and modelled points are of 0.03 mag on average, as reported on each graph.

overplotted to the data. The excellent match of the photometry measured on K2 frames with the shape models illustrate the interest of data mining K2 data archive for SSO period determination and shape modelling.

4 CONCLUSION

We present a new version of the VO web service SkyBoT. Its cone-search method allow us to list all the SSOs present within a given FoV at a given epoch, as visible from the Earth, the ESA *Rosetta* mission, and now the NASA *Kepler* telescope. More space missions can be added upon request, if desired by the community. Typical queries over limited FoVs take less than 10 s, while queries over extended FoV such as *Rosetta*/OSIRIS camera or *Kepler* full CCD array take about a minute. Possible applications of SkyBoT for K2 data are presented, and the results illustrate the interest of K2 for studying asteroids spin, period, and shapes from the light curves which can be extracted from K2 data. Their analysis and interpretation will be presented in a forthcoming paper (Carry et al., in preparation).

ACKNOWLEDGEMENTS

We acknowledges support of the ESAC Faculty for J. Berthier's visit. This research has received funding from the European Union's H2020-PROTEC-2014 – Protection of European assets in and from space project no. 640351 (NEOShield-2). A. Santerne is supported by the European Union under a Marie Curie Intra-European Fellowship for Career Development with reference FP7-PEOPLE-2013-IEF, number 627202. He also acknowledges the support from the Fundação para a Ciência e Tecnologia, FCT (Portugal) in the form of the grants UID/FIS/04434/2013 (POCI-01-0145-FEDER-007672)

and POPH/FSE (EC) by FEDER funding through the program 'Programa Operacional de Factores de Competitividade – COMPETE'.

REFERENCES

Berthier J., Vachier F., Thuillot W., Fernique P., Ochsenbein F., Genova F., Lainey V., Arlot J.-E., 2006, in Gabriel C., Arviset C., Ponz D., Enrique S., eds, ASP Conf. Ser. Vol. 351, Astronomical Data Analysis Software and Systems XV. Astron. Soc. Pac., San Francisco, p. 367

Berthier J. et al., 2009, European Planetary Science Congress. p. 676 (Available at: http://meetings.copernicus.org/epsc2009)

Bonnarel F. et al., 2000, A&AS, 143, 33

Borucki W. J. et al., 2009, Science, 325, 709

Bouy H., Bertin E., Moraux E., Cuillandre J.-C., Bouvier J., Barrado D., Solano E., Bayo A., 2013, A&A, 554, A101

Bowell E., Muinonen K. O., Wasserman L. H., 1993, Proc. IAU Symp. 160, Asteroids, Comets, Meteors. Lunar and Planetary Institute, Houston, TX, p. 44

Bulirsch R., Stoer J., 1966, Numer. Math., 8, 1

Carry B., Snodgrass C., Lacerda P., Hainaut O., Dumas C., 2012, A&A, 544, A137

Carry B., Solano E., Eggl S., DeMeo F. E., 2016, Icarus, 268, 340

Conrad A. R., Goodrich R. W., Campbell R. D., Merline W. J., Drummond J. D., Dumas C., Carry B., 2009, Earth Moon Planets, 105, 115

Delgado A., Delmotte N., Vuong M., 2011, in Evans I. N., Accomazzi A., Mink D. J., Rots A. H., eds, ASP Conf. Ser. Vol. 442, Astronomical Data Analysis Software and Systems XX. Astron. Soc. Pac., San Francisco, p. 111

Durech J. et al., 2009, A&A, 493, 291

Fienga A., Manche H., Laskar J., Gastineau M., Verma A., 2014, Scientific Notes, preprint (arXiv:1405.0484)

Hanuš J. et al., 2011, A&A, 530, A134

Howell S. B. et al., 2014, PASP, 126, 398

Lainey V., Duriez L., Vienne A., 2004a, A&A, 420, 1171

Lainey V., Arlot J. E., Vienne A., 2004b, A&A, 427, 371

Lainey V., Dehant V., Pätzold M., 2007, A&A, 465, 1075

Laskar J., Jacobson R. A., 1987, A&A, 188, 212

Le Guyader C., 1993, A&A, 272, 687

Pál A., Szabó R., Szabó G. M., Kiss L. L., Molnár L., Sárneczky K., Kiss C., 2015, ApJ, 804, L45

Rocher P., Cavelier C., 1996, in Ferraz-Mello S., Morando B., Arlot J.-E., eds, Proc. IAU Symp. 172, Dynamics, Ephemerides, and Astrometry of the Solar System. Kluwer, Dordrecht, p. 357

Sierks H. et al., 2011, Science, 334, 487

Stoer J., Bulirsch R., 1980, Introduction to Numerical Analysis. Springer-Verlag, New York

Szabó R. et al., 2015, AJ, 149, 112

Vaduvescu O., Curelaru L., Birlan M., Bocsa G., Serbanescu L., Tudorica A., Berthier J., 2009, Astron. Nachr., 330, 698

Vaduvescu O., Tudorica A., Birlan M., Toma R., Badea M., Dumitru D., Opriseanu C., Vidican D., 2011, Astron. Nachr., 332, 580

Vaduvescu O. et al., 2013, Astron. Nachr., 334, 718

Vienne A., Duriez L., 1995, A&A, 297, 588

This paper has been typeset from a TEX/LATEX file prepared by the author.